Tellus (2007), 59A, 444–454
Printed in Singapore. All rights reserved

TELLUS

Characteristics of tropical cyclone activity over the eastern North Pacific: the extremely active 1992 and the inactive 1977

By PENG WU and PAO-SHIN CHU*, *Department of Meteorology, School of Ocean and Earth Science and Technology, University of Hawaii at Manoa, 2525 Correa Road, Honolulu, HI 96822, USA*

(Manuscript received 31 August 2006; in final form 26 March 2007)

ABSTRACT

The eastern North Pacific experiences large variability in tropical cyclone (tropical storm and hurricane) frequency from year to year. Large-scale environmental conditions during the peak hurricane season (July, August and September) are contrasted for two extreme years; 1992 is the most active year and 1977 the most inactive year.

Sea surface temperatures in both 1992 and 1977 are warm and favourable for tropical cyclone (TC) formation, whereas other environmental factors undergo pronounced changes over the major development area (MDA) for the two extreme years. For instance, the 1992 hurricane season features weaker vertical wind shear, larger low-level relative vorticity, stronger mid-tropospheric ascending motion, stronger upper-level divergence, and larger mid-tropospheric moisture content than the 1977 hurricane season. These changes correspond well to the variation of the TC activity during the two extreme years.

In addition, a monsoon trough is only present over the MDA in 1992. Convective disturbances within a 4–10-d period propagating consistently from the east bring stronger convection in 1992 than in 1977. In both years, anomalous zonal wind over the MDA oscillates with the intraseasonal timescale. However, TCs do not necessarily form during the westerly phases in either year in the intraseasonal timescale.

1. Introduction

The dynamics of cyclogenesis are non-linear and complicated. Although a well accepted and closed theory is absent, theoretical and observational studies have isolated a number of physical conditions that are important for cyclogenesis. Researches have shown that the frequency and spatial distribution of tropical cyclone (TC) formation are closely related to some environmental factors on the seasonal timescale. These factors predict favourable pattern for cyclogenesis when the necessary physical conditions are satisfied in the environment.

Gray (1977) summarized six environmental factors that are related to the seasonal climatology of cyclogenesis. These factors include the Coriolis force, low-level relative vorticity, vertical wind shear (VWS) between the upper and lower troposphere, warm sea surface temperatures (SSTs), moist instability in terms of the vertical gradient of equivalent potential temperature (θ_e), and moderately high relative humidity in the middle troposphere. The first three factors can be combined to form a single term called the dynamic potential, and the last three factors are related to a term called the thermal potential. The product of these two terms is referred to as the seasonal genesis parameter (SGP). The diagnosed seasonal cyclogenesis over the western North Pacific (WNP) using the SGP derived by Gray (1977) was quite similar to the observation.

Other studies have also shown skill employing Gray's SGP in the diagnosis of cyclogenesis. Watterson et al. (1995) examined the climatology and interannual variation of global cyclogenesis with SGP derived from the general circulation model (GCM). Clark and Chu (2002) studied interannual variation of TC activity over the central North Pacific and found the dynamic potential values of SGP are two to three times greater in the El Niño composite than in the La Niña composite.

The influence of the El Niño phenomenon on the TC activity in the eastern North Pacific (ENP) has been the subject of several studies and is reviewed by Chu (2004). The overall TC frequency over the ENP does not change appreciably from the El Niño to La Niña events (Whitney and Hobgood, 1997). However, the number of intense hurricanes (maximum wind speeds of at least 50 m s^{-1}) during El Niño years increases by a factor of two compared to that during La Niña years (Chu, 2004). Other noteworthy features include westward shifts of TC genesis

*Corresponding author.
e-mail: chu@hawaii.edu
DOI: 10.1111/j.1600-0870.2007.00248.x

location and longer TC life span during El Niño years as opposed to La Niña years (Irwin and Davis, 1999; Kimberlain, 1999; Chu, 2004).

Based on a Bayesian changepoint analysis, the hurricane activity over ENP during the last 30 yr has been shown to have undergone decadal variations with two abrupt phase shifts occurring around 1982 and 1999 (Zhao and Chu, 2006). Accordingly, the epoch 1972–1981 is characterized by an inactive phase, the 1982–1998 epoch an active phase, and the 1999–2003 epoch an inactive period. A lower number of major hurricanes is predicted for the decade 2004–13 given the recent inactive period of hurricane activity (Zhao and Chu, 2006).

The TC formation in the ENP shows a pronounced annual cycle (McBride, 1995). The official season defined by the U.S. National Weather Service extends from May 15 to November 30, with the peak season from July to September, when more than 70% of TCs are observed. The ENP also experiences large variations in TC counts from year to year. For example, only five named storms were reported in the peak season of 1977 but 17 occurred in the peak season of 1992, a difference by a factor of more than three between these two extreme years. This contrast is also reflected in the Accumulated Cyclone Energy (ACE) index (e.g. Bell et al., 2000; Camargo and Sobel, 2005). The ACE index is here defined as the sum of the squared 6-hourly maximum sustained wind speed for all named storms for a single season. For the period from 1966 to 2003 (a total of 38 yr), 1977 is marked by a minimum ACE and 1992 has a maximum ACE.

Section 2 introduces the data employed in this study. Section 3 discusses the climatology of cyclogenesis and long-term environmental conditions over the ENP. Section 4 contrasts the variations of the environmental conditions between 1992 and 1977, and Section 5 discusses other circulation features. The influence of TC on the seasonal mean relative vorticity is discussed in Section 6. Lastly, a summary is in Section 7.

2. Data

For TCs, we use the best track data set for the ENP from Tropical Prediction Center (TPC)/National Hurricane Center (NHC). The data set records 6-hourly (0000, 0600, 1200 and 1800 UTC) centre locations and intensities (maximum 1-min surface wind speeds) for all tropical storms (maximum sustained surface wind speeds between 17.5 and 33 m s^{-1}) and hurricanes (wind speeds at least 33 m s^{-1}) from 1966 to 2003. In this study, TC refers to tropical storms and hurricanes. Observation of TCs is considerably better in the post-satellite era than in the pre-satellite era. In this study, we choose to examine the period from 1966 to 2003 because routine satellite surveillance started in 1966 over the ENP (Lawrence and Rappaport, 1994).

Daily averaged wind, air temperature, specific humidity at the surface and several pressure levels, geopotential height at 925 hPa, relative humidity and vertical velocity at 500 hPa, and sea level pressure (SLP) are derived from the National Center for Environmental Prediction-National Center for Atmospheric Research (NCEP-NCAR) reanalysis data set (Kalnay et al., 1996; Kistler et al., 2001). The horizontal resolution of the reanalysis data is 2.5° latitude–longitude.

Monthly mean SSTs are taken from National Oceanic and Atmospheric Administration's (NOAA) Extended Reconstructed data provided through the Climatic Diagnostic Center (CDC) in Boulder, Colorado; SST data are available with horizontal resolution of 2° latitude–longitude. For details of SST data, see Smith et al. (1996).

Daily averaged outgoing longwave radiation (OLR) with 2.5° latitude–longitude resolution is derived from the NOAA Interpolated OLR data set which provided through the CDC (http://www.cdc.noaa.gov/cdc/data.interp_OLR.html). The temporal coverage is from 1974 to present, with data missing for 1978.

The vertical component of the relative vorticity is calculated from the NCEP-NCAR reanalysis wind fields with finite differentiation using the Grid Analysis and Display System (GrADS).

3. Climatology of cyclogenesis and seasonal mean environmental conditions

Figure 1 shows the initial detection locations of TCs that occurred during the peak hurricane seasons (JAS) of the 38-yr period. Historically, about 95% of the total TC formations were observed in the region extending from 90°W to 120°W and from 10°N to 20°N (denoted with solid lines). In the following sections, this region is referred to the major development area (MDA).

Climatological mean SSTs during the peak hurricane season are >28 °C over most of the MDA, while the standard deviation of the seasonal mean is <0.5 °C. With the very warm background SST and a very small deviation from year to year, SSTs in the MDA are expected to remain >26.5 °C during the peak season, a widely accepted empirical threshold for TC formation (McBride, 1995). Long-term seasonal mean low-level relative vorticity at 925 hPa is about 4×10^{-6} s^{-1} over the MDA. The

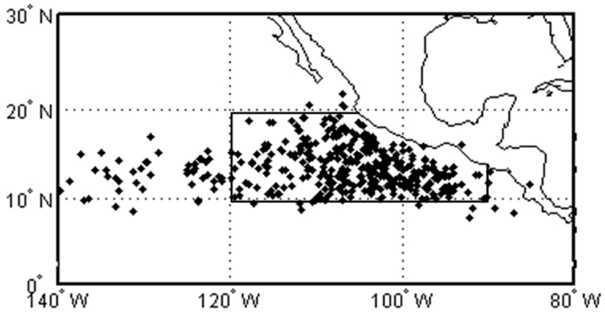

Fig. 1. Initial detection locations of tropical cyclones (based on best track data) during the peak hurricane season (July–September) of 1966–2003. The major development area (MDA) is denoted by thick lines.

relative humidity in the mid-troposphere (500 hPa) exhibits a local maximum with a value of >50% over the MDA. Vertical wind shear (VWS) is defined as the magnitude of the difference between the zonal and meridional wind at the 200 and 850 hPa and is given by the equation

$$\mathrm{VWS} = \left[(u_{200\mathrm{hPa}} - u_{850\mathrm{hPa}})^2 + (v_{200\mathrm{hPa}} - v_{850\mathrm{hPa}})^2\right]^{1/2}. \quad (1)$$

The long-term seasonal average of VWS is about 6 m s^{-1} over the MDA, which is smaller than the critical vertical shear line, 10 m s^{-1}, for TC intensification. Given a weak VWS, moist mid-troposphere, warm SSTs, and the presence of strong cyclonic relative vorticity in the lower troposphere, seasonal mean environmental conditions are certainly conducive for TC formation over the MDA. These results agree with McBride (1995) who suggested that the highest frequency of cyclogenesis per unit area in the world is found over a compact region in the ENP.

4. Variations of the seasonal mean environmental conditions for 1992 and 1977

4.1. SST

Tropical cyclones form and develop over regions with very warm sea surface, where warm and moist air is available to support the sustained deep convection and organized convective circulation with great intensity. Although 12 more TCs formed during the hurricane season in 1992 than 1977, the difference of seasonal mean SSTs between these 2 yr is negligible over the MDA (figure not shown). This suggests that the background SST is sufficiently warm for these two contrasting years and factors other than SSTs must be sought to account for the enhanced TC activity in the 1992 hurricane season and the suppressed TC activity in 1977.

4.2. Mid-tropospheric moisture content and conditional instability

Figure 2 shows that the difference of the seasonal mean 500 hPa relative humidity for 1992 and 1977 averages around 14% over the MDA. This value is more than one fourth of the long-term seasonal average (50%). Therefore, larger moisture content in the mid-troposphere is related to the higher TC activity in 1992.

One of the environmental factors given by Gray (1977) is the moist instability, which is defined as the vertical gradient of equivalent potential temperature (θ_e). For the sake of computational convenience, we employ the moist static energy (MSE) that has the same physical meaning as θ_e to measure the moist instability. The MSE is calculated as $C_pT + gz + L_vq$, in which each term stands for the enthalpy, gravitational potential energy, and latent heat content of an air parcel, respectively. Also note that L_v is the latent heat of vaporization, and q is the specific humidity.

The vertical profile of the seasonal mean MSE averaged over the MDA is shown in Fig. 3. During the hurricane seasons of

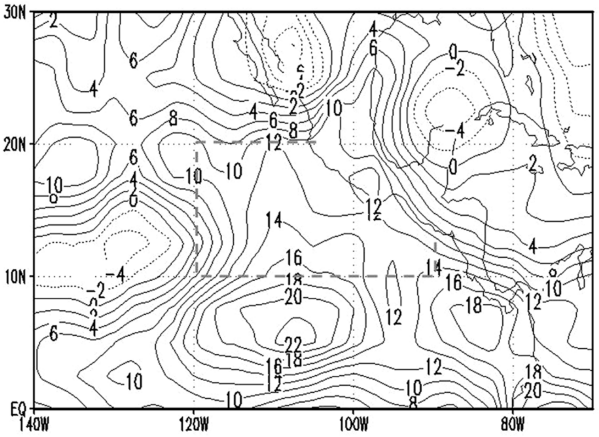

Fig. 2. 1992 minus 1977 seasonal mean 500 hPa relative humidity (%). Solid (dashed) contours denote positive (negative) values. The MDA is denoted by grey dashed lines hereafter.

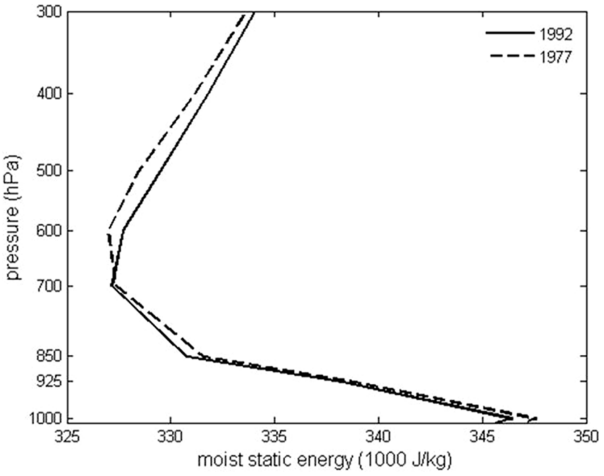

Fig. 3. Vertical profile of seasonal mean moist static energy averaged over 90–120°W and 10–20°N in 1992 (solid) and 1977(dashed).

1992 and 1977, the troposphere below 700 hPa reveals comparable conditional instability with the MSE increasing with height. However, starting from 700 hPa, MSE in 1992 is greater than that in 1977, and the difference attains its maximum at 500 hPa. Higher MSE at the 500 hPa level in 1992 is consistent with the greater moisture content reflected in Fig. 2. To test the significance of the 500 hPa seasonal mean MSE difference, daily MSE values during the two contrasting hurricane seasons are used. The goodness-of-fit test (Wilks, 1995) indicates that all the points, consisting of an observed value and the theoretical estimate derived from the cumulative density function of a Gaussian distribution, fall close to the 1:1 line in a quantile–quantile plot (not shown). Thus, the data of MSE follow the Gaussian distribution quite well. A two-sample t test for the difference of the seasonal mean of the 500 hPa MSE under serial dependence is then performed; with a p-value of 0.04, a one-sided test rejects

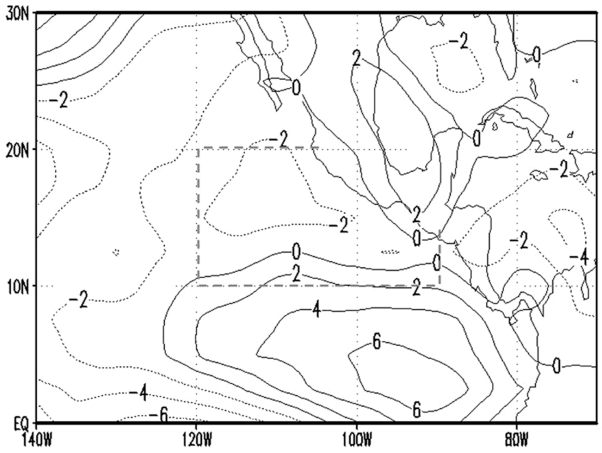

Fig. 4. 1992 minus 1977 seasonal mean vertical wind shear (m s^{-1}) between 200 and 850 hPa. Solid (dashed) contours denote positive (negative) values.

the null hypothesis of no difference in the mean between 1992 and 1977 at the 5% test level.

4.3. Vertical wind shear

Figure 4 shows the difference of the seasonal mean VWS between 1992 and 1977. The negative values over the MDA suggest that weaker VWS is present in the hurricane season of 1992, which is more favourable for cyclogenesis than the 1977 case. Additionally, the difference over the MDA is as large as 2 m s^{-1}, which accounts for approximately one third of the long-term seasonal average.

4.4. Low-level cyclonic vorticity and vertical coupling for deep convection

Low-level cyclonic vorticity is considered as another critical environmental factor for cyclogenesis (Gray, 1977). The vorticity maximum is usually located along the monsoon trough. Figure 5 shows the streamline analysis based on 925 hPa seasonal mean winds during the hurricane seasons of 1992 and 1977. In 1992, a well-established monsoon trough marked by the bold solid curve is observed over the MDA, whereas monsoon trough is absent or at least not well defined over that area in 1977.

Differences of the seasonal mean circulation at the 925, 500 and 200 hPa levels between 1992 and 1977 are shown in Fig. 6. Relative vorticity at the 925 hPa is higher in 1992 than in 1977 over the MDA with the difference being about 6×10^{-6} s^{-1} (Fig. 6a). This difference exceeds the climatological seasonal mean value by 50%. The well-established monsoon trough in 1992 is consistent with the greater low-level cyclonic vorticity (Fig. 6a) and weaker VWS (Fig. 4) within the same area. In particular, the area of the positive vorticity difference in Fig. 6a approximately follows the monsoon trough (Fig. 5). Negative

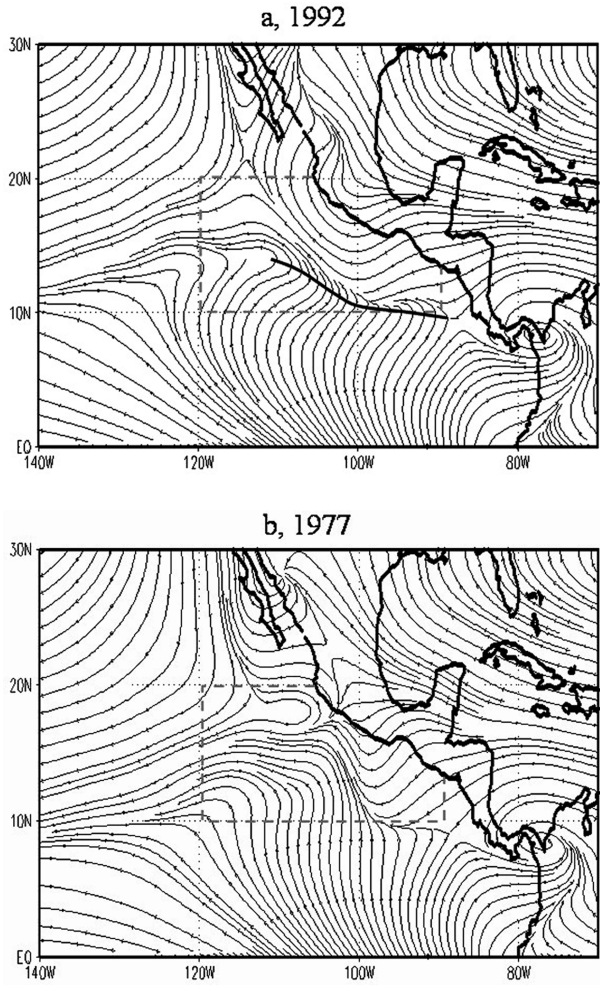

Fig. 5. Seasonal mean 925 hPa streamline in (a) 1992 and (b) 1977. Monsoon trough is denoted by the bold solid curve in (a).

values in Fig. 6b suggest that ascending motion at the 500 hPa level is greater in 1992 over a large area that includes the MDA. At the 200 hPa level, Fig. 6c shows that divergent flow is also stronger in 1992 over an area to the south of the MDA. Corresponding to the high TC activity in 1992, circulations at the three levels constitute the vertical coupling that is favourable for deep convection to form, although a southward tilt with height is present in this vertical coupling structure.

5. Other prominent circulation features

A number of factors studied above have constituted a favourable (unfavourable) seasonal mean environment for cyclogenesis in the 1992 (1977) hurricane season. To some extent, these conditions are all directly related to the physical requirement for cyclogenesis. In the following, we will examine other features

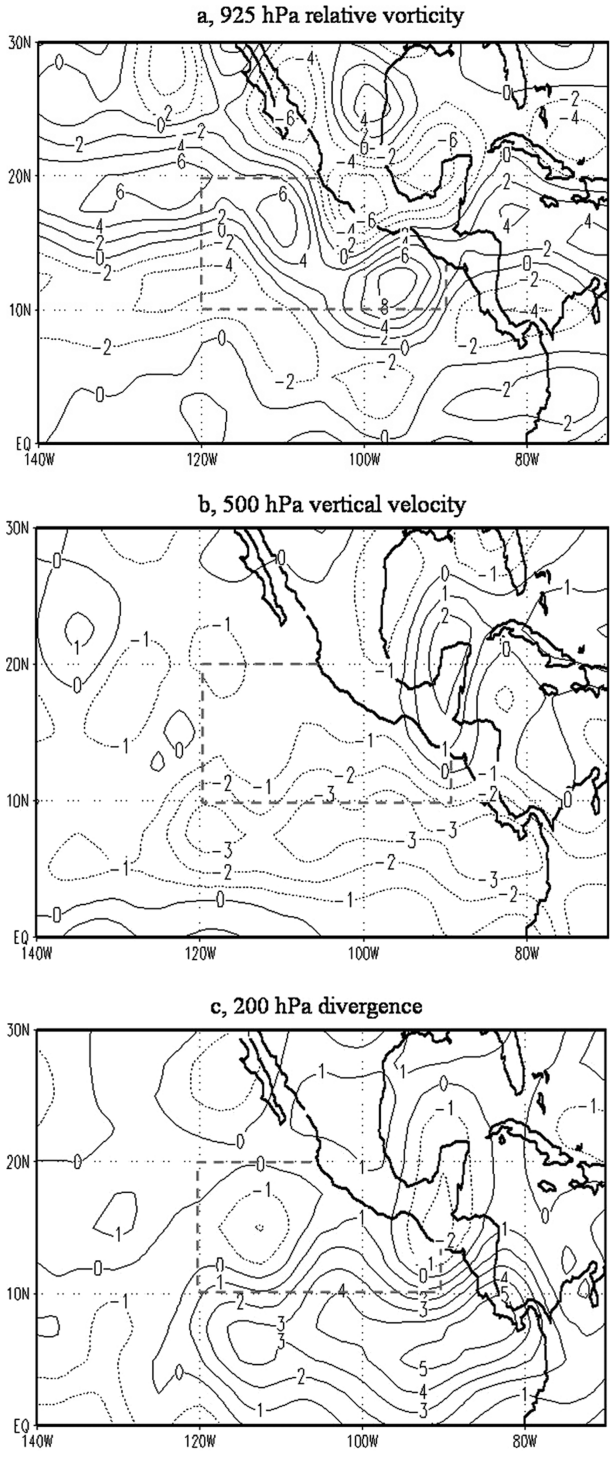

Fig. 6. Difference (1992 minus 1977) of seasonal mean 925 hPa relative vorticity (10^{-6} S^{-1}) (a), 500 hPa vertical velocity (10^{-2}Pa s^{-1}) (b) and 200 hPa divergence (10^{-6} S^{-1}) (c). Solid (dashed) contours denote positive (negative) values.

that are not directly related to TC formation, but might contribute to the variation of the environment.

5.1. Westward extension of the subtropical ridge over the Atlantic

Returning to Fig. 5a, one distinct feature other than the monsoon trough is the presence of a ridge around 100°W on the poleward side of the trough. Although the 925 hPa streamline analysis should be masked out over some parts of the Central American landmass due to elevated topography, the easterly ridge still dominates over the ocean off the western coast of Central America. We speculate that the westward extension of the Atlantic subtropical ridge might contribute to the formation of the easterly ridge associated with the monsoon trough in 1992. The difference of the seasonal mean geopotential height and wind at the 925 hPa level between 1992 and 1977 over a larger domain is shown in Fig. 7. Westward extension of the subtropical ridge is detected over the Gulf of Mexico and part of Central America, where an area of positive geopotential height difference and anticyclonic difference of the circulation is centred near 20°N and 90°W. The extension of subtropical ridge over this area in the 1992 hurricane season is consistent with the easterly ridge observed in Fig. 5a. Therefore, the westward extension of the Atlantic subtropical ridge is associated with the favourable circulation pattern for cyclogenesis over the ENP.

5.2. Westward propagating convective disturbances

It has been suggested that cyclogenesis in the ENP often occurs in association with synoptic-scale easterly waves that propagated from Africa across the Atlantic and Caribbean (Avila, 1991). Given the westward extension of the subtropical ridge as revealed in the seasonal mean map in 1992 (Fig. 7), it is natural to ask the role of these easterly waves on cyclogenesis in both 1992 and 1977. Burpee (1972) showed that the easterly waves developed over Africa where the negative meridional gradient of potential vorticity (PV) near 700 hPa offered an unstable basic state. Likewise, Molinari et al. (1997) demonstrated the negative PV gradient offered an unstable basic state to reinvigorate the easterly waves propagating westward in the summer of 1991. These re-energized easterly wave packages are blocked by the Sierra Madre Mountain of Mexico and divert to the south of the mountain range (Mozer and Zehnder, 1996). Conservation of potential vorticity results in the formation of a barotropically unstable low-level jet which provides a background for the generation of the vorticity maximum downstream of the mountain. This mechanism is used to account for tropical cyclogenesis in the ENP (Mozer and Zehnder, 1996).

In view of the potential importance of these waves, we are interested in knowing how active are these transient convective disturbances from the east, what are their preferred periods, and what are their temporal phase relations with TC development

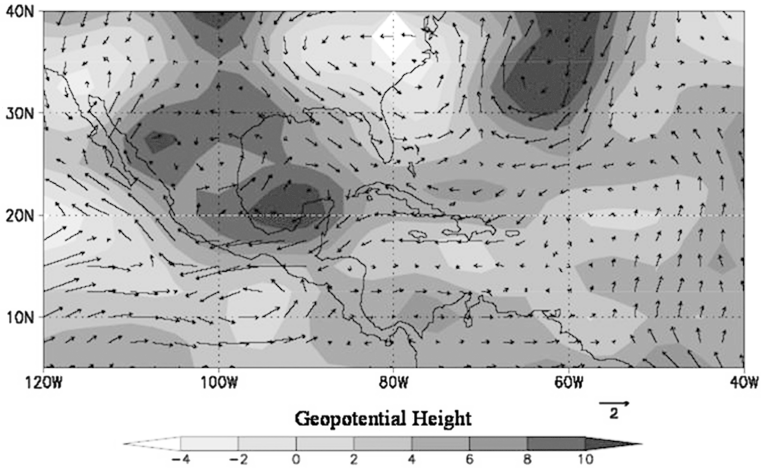

Fig. 7. Difference of the seasonal mean 925 hPa geopotential height (m) and wind between 1992 and 1977.

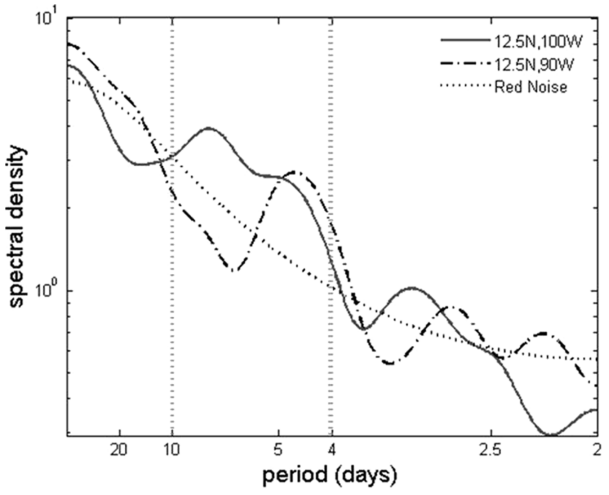

Fig. 8. Spectral density functions of OLR during June–October in 1992 over (12.5°N, 100°W) and (12.5°N, 90°W). Dotted curve denotes the red noise spectrum.

for two extreme seasons? To pinpoint the preferred timescales of disturbances, spectral analysis is used. Following the method of Chu and Katz (1989), spectral densities are calculated based on time series of the unfiltered daily OLR during June–October for two locations where seasonal mean convection is strong and variances are large (figures not shown). These two locations are 12.5°N, 100°W and 12.5°N, 90°W, all in the MDA. In Fig. 8, spectral density functions of the disturbances have higher amplitudes relative to the red noise spectrum over 4–10-d periods. Therefore, it becomes evident that it is the synoptic scale disturbances with 4–10-d periods that are related to the stronger convective activity in 1992.

Subsequently, time-longitude cross sections of the 4–10-d filtered OLR anomalies averaged between 10 and 20°N are plotted in Fig. 9 for the period of June to October in 1992 and 1977. In both panels a and b, each convective disturbance passing over the cyclogenesis region between 90°W and 120°W could be traced back to 80°W or farther. Meanwhile, each TC formation denoted by the solid dot is preceded by such a disturbance package propagating westward. Based on these features, we suggest that it is the 4–10-d convective disturbances propagating from the east of the MDA that are related to the more active convection in 1992. This seems to be consistent with Molinari et al. (1997) and Molinari and Vollaro (2000) analyses of the 1991 hurricane season.

5.3. Zonal wind oscillation with MJO timescale

On the intraseasonal timescale, Madden-Julian Oscillation (MJO) modulates cyclogenesis while alternating low-level easterly and westerly winds over the area between the equator and 15°N in the ENP (Maloney and Hartmann, 2000). The composited zonal wind anomalies during the westerly phases are depicted by westerly anomalies to the south of easterly anomalies, thereby creating a cyclonic vorticity favourable for TC activity. In view of the potential influence of intraseasonal oscillation on the background wind field, it is reasonable to examine whether MJO is attributable to the high TC activity in the 1992 hurricane season.

In order to follow the characteristic periods of MJO, a 30–50-d bandpass filter is first used for zonal winds at 850 hPa, where MJO has the strongest signal (Madden and Julian, 1994). Since amplitude of oscillation could be reflected by variance of the underlying variable, we plot the variances of the filtered zonal winds during the hurricane seasons in Fig. 10. In 1992, the maximum variance (12.5°N, 114°W) is located farther northwestward than that in 1977 (10°N, 105°W).

Figure 11 shows the time series of the 30–50-d filtered zonal wind anomalies from June to October over the region where the maximum variances are observed (Fig. 10). The time series show oscillation with period of MJO timescale. In both 1992

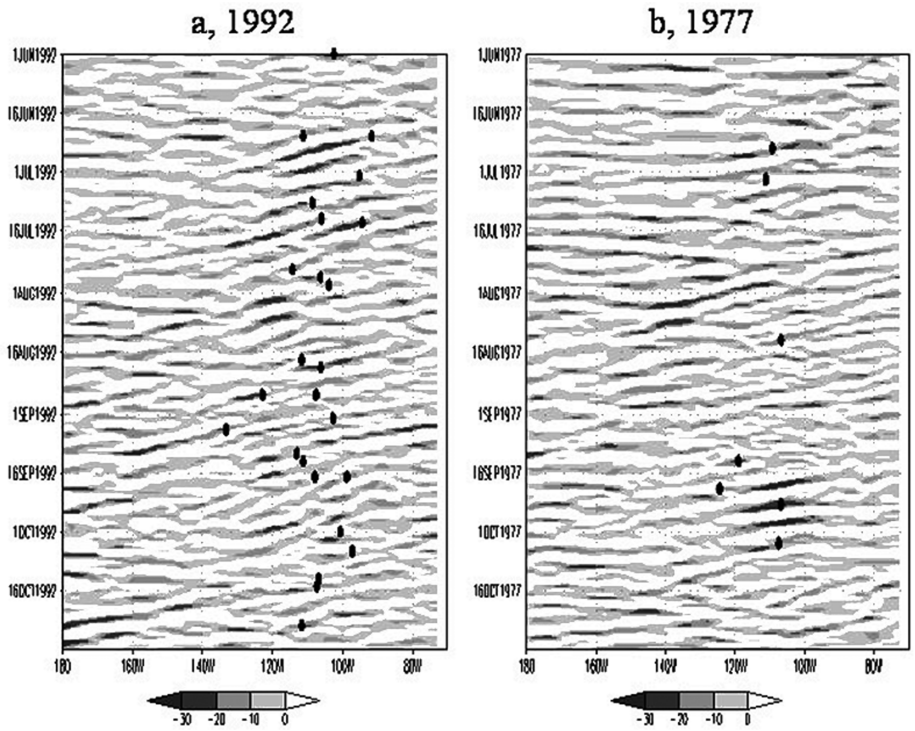

Fig. 9. Time-longitude cross sections of 4–10-d filtered outgoing longwave radiation anomalies (W m^{-2}) averaged between 10 and 20°N in 1992 (a) and 1977 (b). Areas with negative values are shaded. Solid dots denote timing and longitudes of cyclogenesis.

and 1977, westerly wind anomalies occur around mid-August and late September, and easterly anomalies occur during early September and mid-October. Although zonal wind anomalies show similar progressing pattern, cyclogenesis indicated by solid squares occur much more frequently in 1992 than in 1977. Additionally, cyclogenesis in 1992 tends to be widespread instead of being clustered and preceded by the peak of westerly zonal wind anomalies. In 1977, cyclogenesis starts during mid-September when anomalous zonal wind is still in the easterly phase.

If westerly wind bursts lead to cyclogenesis, then we would expect a totally different scenario where cyclogenesis would cluster and be preceded by the peaks of westerly anomalies. However, this is not true in Fig. 11. Thus westerly wind bursts with the MJO timeframe should not be taken as the direct cause of cyclogenesis for these 2 yr.

To support this point, we plot in Fig. 12 the time-longitude cross-section of the 30–50-d filtered 850 hPa zonal wind anomalies. The cross sections are located along 12.5°N for 1992 and 10°N for 1977. These are the latitudes where the maximum variances are observed in the 2 yr (Fig. 10). In both panels of Fig. 12, westerly anomalies do not precede TC formation in time, especially for the strong westerly anomalous events around July 16, August 20, and September 16 in 1992. Besides, westerly anomalies with larger amplitudes and extension in both time and space occur in the 1977 hurricane season, when cyclogenesis frequency is significantly lower.

Although 850 hPa zonal winds do show oscillation with the MJO timescale, and such oscillation has larger amplitude in 1992 than in 1977, cyclogenesis does not conform to the westerly phase of the anomalous zonal winds in either 1992 or 1977. Therefore, the westerly wind anomalies at the low levels on the MJO timescale do not have a clear relationship with cyclogenesis for the 2 yr selected in this study.

6. TC influence on the seasonal mean relative vorticity

In the previous section, we have shown that larger cyclonic relative vorticity (Fig. 6a) and a well-established monsoon trough (Fig. 5a) are present at the 925 hPa level in 1992. Given they are closely located, these two features are considered to be related to each other. However, since TCs always breed in an environment where low-level cyclonic vorticity is strong, there exists the possibility that the seasonal mean cyclonic vorticity over the MDA is produced by TCs themselves. To test such possibility, we next examine the seasonal mean vorticity field in which the influence from TCs has been removed. To accomplish this, we remove TC influence in two separate approaches. For the first one, in a way similar to Chu (2002) for the central North Pacific, we examine a period during the pre-season when there were no TCs over the ENP. Independently, for the second approach, we artificially remove the

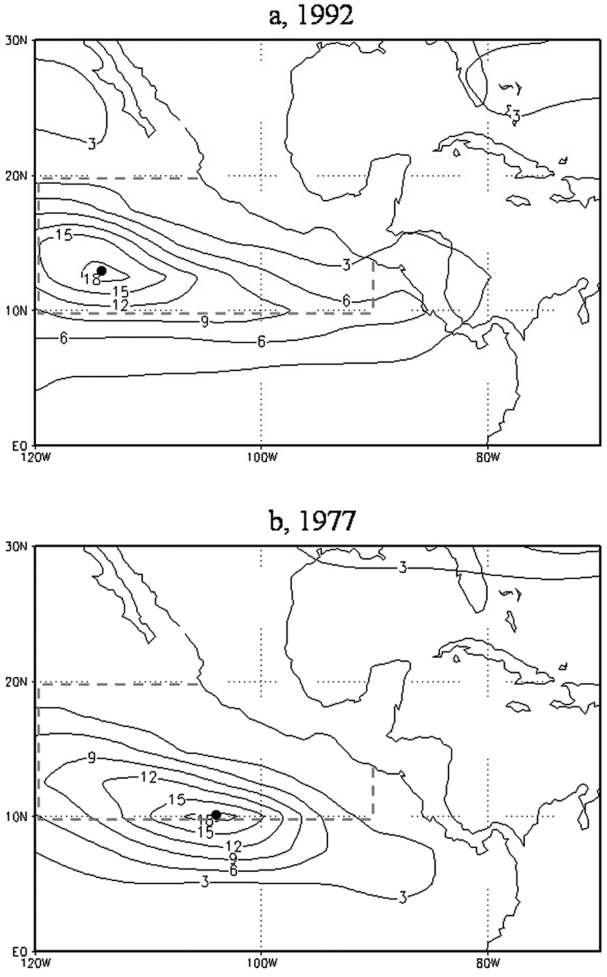

Fig. 10. Variance ($m^2\ s^{-2}$) of 30–50-d filtered 850 hPa zonal wind anomalies during July–September in (a) 1992 and (b) 1977. Solid dots denote locations of maximum values in each year.

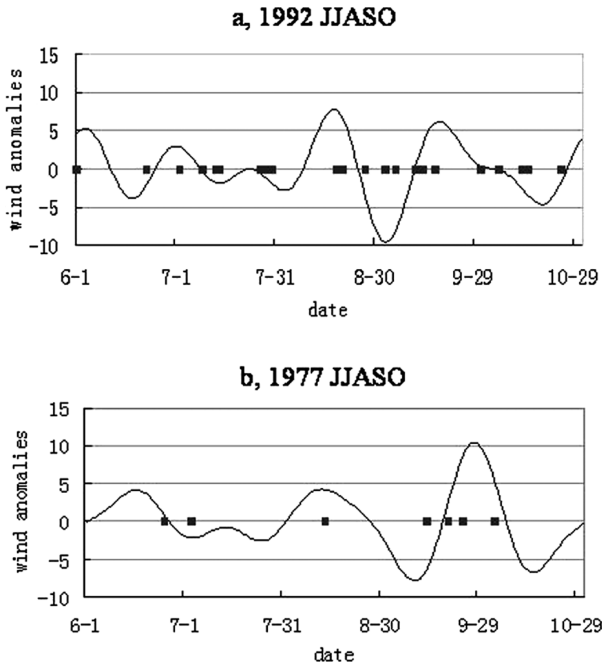

Fig. 11. Time series of 30–50-d filtered 850 hPa zonal wind anomalies ($m\ s^{-1}$) during June to October in (a) 1992 and (b) 1977 over the locations denoted by the solid dots in Fig. 10. Solid squares denote the timing of cyclogenesis.

TC-like vortex based on the reanalysis data using a three-point smoothing.

Figures 13 and 14 show the 925 hPa streamline and relative vorticity for the period (June 5–June 21) when no TCs were present over the ENP in either 1992 or 1977. During the pre-season period in 1992, monsoon trough and cyclonic vorticity are observed over the southeastern portion of the MDA (between 90°W and 100°W along 10°N) in Fig. 13. During the pre-season period in 1977, the monsoon trough is not observed and the cyclonic vorticity is very weak in the MDA (Fig. 14). Thus it becomes evident that, without the influence from TC activity, cyclonic vorticity is closely related to the monsoon trough during the pre-season period. Assuming the atmospheric state is persistent, TCs had very limited influence on the seasonal mean cyclonic vorticity over the MDA in either 1992 or 1977.

This argument is further verified in a separate analysis, in which the TC-like vortex is removed from the seasonal mean field with a three-point smoothing operator following Kurihara et al. (1993). This is performed using the daily wind fields during the hurricane seasons of 1992 and 1977. Specifically, on any day when TC is reported according to the best track data, the smoothing operator is applied toward the winds at the 16 gridpoints surrounding the TC centre, with four on the zonal and four on the meridional direction. To show the quality of the smoothing, the relative vortivity based on the original and the smoothed winds at the 925 hPa level is analysed for September 15 1992 (figure not shown). On this day, Hurricane Roslyn (September 13–September 25) is centred at 18°N and 113°W, where cyclonic vorticity larger than $50 \times 10^{-6}\ s^{-1}$ is observed. After the smoothing, the largest cyclonic vorticity over that region is reduced to $30 \times 10^{-6}\ s^{-1}$, with its contour being located on average 250 km away from the hurricane center. Thus, the smoothing is able to remove the TC-like vortex, and the environmental cyclonic vorticity is unchanged. However, the smoothed seasonal mean 925 hPa relative vorticities are basically unchanged from the original fields in both 1992 and 1977. Therefore, TC influence on the seasonal mean vorticity field is trivial.

7. Summary

Seasonal mean environmental conditions are compared for 1992 and 1977, which experience the most active and inactive TC

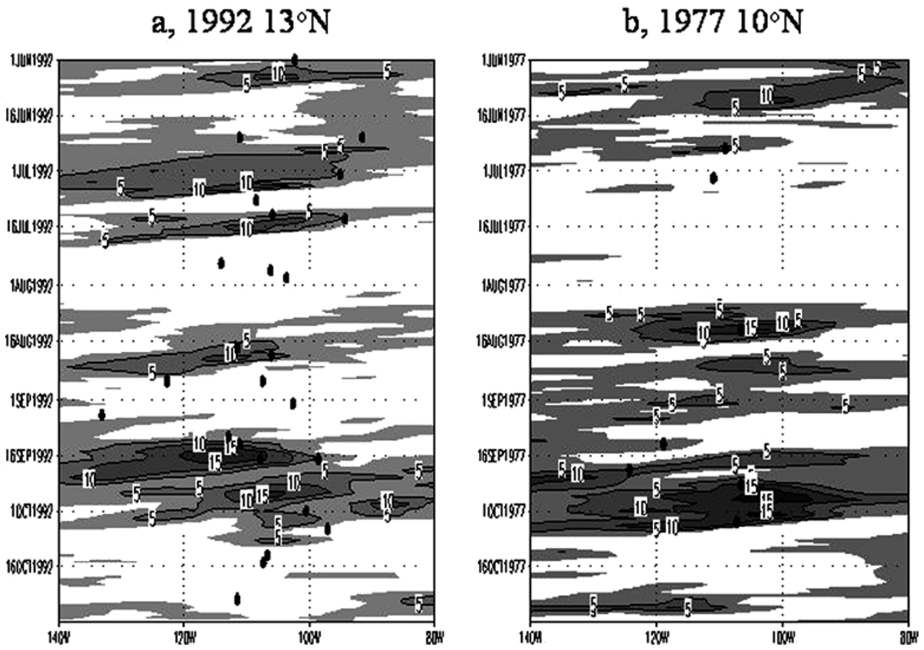

Fig. 12. Time-longitude cross section of 850 hPa zonal wind anomalies during June to October in (a) 1992 along 13°N and (b) 1977 along 10°N. Only positive values are shown and shaded. Contours are every 5 m s^{-1}. Solid dots denote the timing and longitudes of cyclogenesis.

activity during a 38-yr period. SSTs are consistently warm and favourable for TC formation. However, large low-level cyclonic vorticity, strong mid-level ascending motion, and upper-level divergence constitute vertical coupling that is indicative for deep convection over the MDA in 1992. The increase of the background low-level relative vorticity would help spin up TCs by increasing moisture convergence and by entraining potential vorticity into TCs (Wang and Chan, 2002). These changes in the environment would enhance (suppress) cyclogenesis in 1992 (1977). Meanwhile, a well-established monsoon trough over the MDA is observed between the enhanced easterlies and cross equatorial westerlies in 1992. The potential impact of TCs on the low-level relative vorticity was investigated with two different approaches by examining a period when there were no TCs and by removing TC-like vortex. It is found that the enhanced cyclonic vorticity over the ENP in 1992 is not likely a response to more TC activity.

Compared with 1977, convective disturbances with 4–10-d periods propagating from the east bring stronger convection on both seasonal mean and transient states in 1992. This result seems to agree with a case study by Molinari et al. (1997) in that synoptic-scale easterly waves over the Caribbean are energized by the unstable lower atmosphere resulted from a sign reversal in the meridional PV gradient. As a wave approaches the Sierra Madre of Mexico from the east, the relative vorticity in the lee increases because the wave is being modified by topography (Mozer and Zehnder, 1996). Consequently, the production of maximum vorticity downstream from the mountain may intensify initial disturbances to tropical cyclones in the ENP. We speculate that the active 1992 hurricane season is attributable to the westward extension of the subtropical ridge over the Atlantic, which tends to steer consistently synoptic-scale convective disturbances over the MDA (Figs. 7 and 9). Upon reaching a region of favourable seasonal mean environmental conditions for TC, these easterly wave disturbances are conducive for the initiation of cyclogenesis in the ENP.

In both 1992 and 1977, anomalous zonal wind over the MDA oscillates with MJO timescale. However, in contrast to a composite study by Maloney and Hartmann (2000), TCs do not necessarily form during the westerly phases in the MJO timescale in this study. For the sake of simplicity, we only selected two points in the MDA where amplitude of oscillation is largest to investigate phase relations of the filtered 850 hPa zonal wind oscillations with cyclogenesis. A more comprehensive study involving the entire tropical ENP is needed in the future to ascertain the potential MJO modulations on low-level zonal wind and the corresponding vorticity fields in 1992 and 1977.

8. Acknowledgments

We are grateful to one anonymous reviewer for numerous constructive comments and criticisms. Thanks are also due to Yuqing Wang and Yi-Leng Chen for their suggestions. This paper was funded in part by NOAA grant NA17RJ1230.

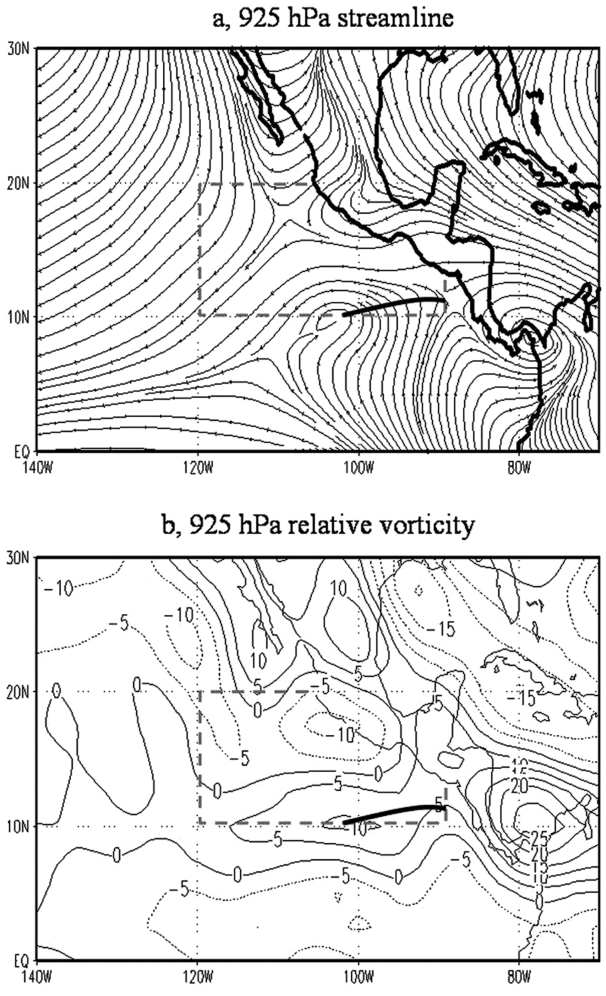

Fig. 13. 925 hPa streamline (a) and relative vorticity in 10^{-6} s^{-1} (b) averaged during June 5 to June 21 in 1992. Bold solid curve denotes the cyclonic wind shear similar with monsoon trough.

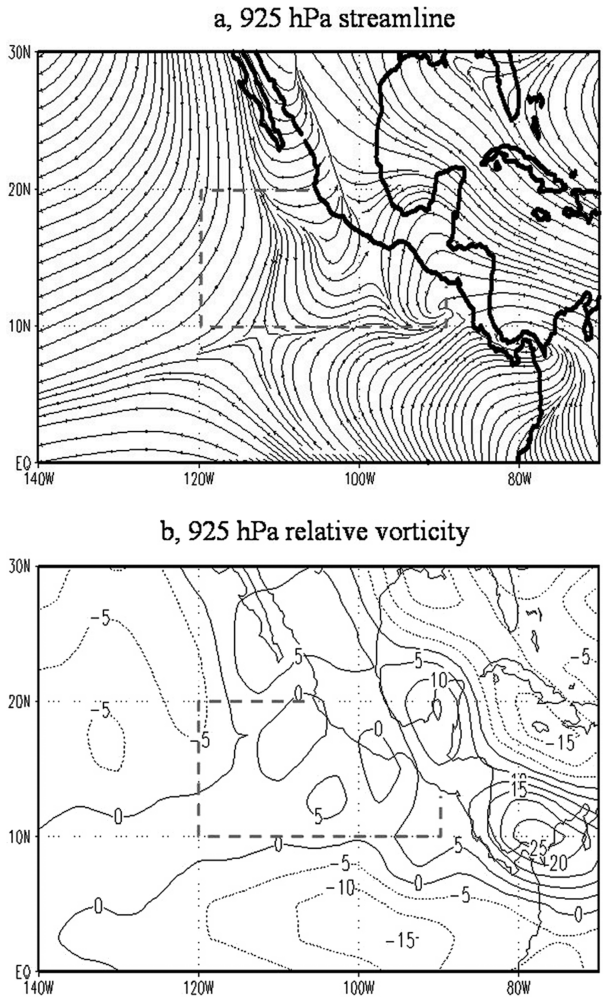

Fig. 14. Same as Fig. 13, except for 1977.

References

Avila, L. A. 1991. Eastern North Pacific hurricane season of 1990. *Mon. Wea. Rev.* **119**, 2034–2046.

Bell, G. D. and Co-authors. 2000. Climate assessment for 1999. *Bull. Amer. Meteor. Soc.* **81**, S1–S50.

Burpee, R. W. 1972. The origin and structure of easterly waves in the lower troposphere of North Africa. *J. Atmos. Sci.* **29**, 77–90.

Camargo, S. J. and Sobel, A. H. 2005. Western North Pacific tropical cyclone intensity and ENSO. *J. Climate* **18**, 2996–3006.

Chu, P.-S. 2002. Large-scale circulation features associated with decadal variations of tropical cyclone activity over the Central North Pacific. *J. Climate* **15**, 2678–2689.

Chu, P.-S. 2004. ENSO and tropical cyclone activity. In: *Hurricanes and Typhoons: Past, Present, and Future*. (edsR. J. Murnane and K.-B. Liu). Columbia University Press, New York, 297–332.

Chu, P.-S. and Katz, R. W. 1989. Spectral estimation from time series models with relevance to the Southern Oscillation. *J. Climate* **2**, 86–90

Clark, J. D. and Chu, P.-S. 2002. Interannual variation of tropical cyclone activity over the central North Pacific. *J. Meteor. Soc. Japan* **80**, 403–418.

Gray, W. M. 1977. Tropical cyclone genesis in the western North Pacific. *J. Meteor. Soc. Japan* **55**, 465–482.

Irwin, R. P. and Davis, R. E. 1999. The relationship between the Southern Oscillation index and tropical cyclone tracks in the eastern North Pacific. *Geophys. Res. Lett.* **20**, 2251–2254.

Kalnay, E. and Coauthors. 1996. The NCEP/NCAR 40-Year Reanalysis Project. *Bull. Amer. Meteor. Soc.* **77**, 437–471.

Kimberlain, T. B. 1999. The effects of ENSO on North Pacific and North Atlantic tropical cyclone activity. *Proc. 23rd Conference on Hurricanes and Tropical Meteorology*, Dallas, Texas, Amer. Meteor. Soc., Boston, 250–253.

Kistler, R. and Coauthors. 2001.The NCEP-NCAR 50-Year Reanalysis: monthly means CD-ROM and documentation. *Bull. Amer. Meteor. Soc.* **82**, 247–267.

Kurihara, Y., Bender, M. A. and Ross, R. J. 1993. An initialization scheme of hurricane models by vortex specification. *Mon. Wea. Rev.* **121**, 2030–2045.

Lawrence, M. B. and Rappaport, E. N. 1994. Eastern North Pacific hurricane season of 1992. *Mon. Wea. Rev.* **122**, 549–558.

Madden, R. A. and Julian, P. R. 1994. Observations of the 40-50-day tropical oscillation—a review. *Mon. Wea. Rev.* **12**, 814–837.

Maloney, E. D. and Hartmann, D. L.,2000. Modulation of eastern North Pacific hurricanes by the Madden-Julian oscillation. *J. Climate* **13**, 1451–1460.

McBride, J. L. 1995. Tropical cyclone formation. In: *Global Perspectives on Tropical Cyclones* (edsR. L. Elsberry). WMO Tech. Document 693, 63–105.

Molinari, J., Knight, D., Dickison, M., Vollaro, D. and Skubis, S. 1997. Potential vorticity, easterly waves, and Eastern Pacific tropical cyclogenesis. *Mon. Wea. Rev.* **125**, 2699–2708.

Molinari, J. and Vollaro, D. 2000. Planetary- and synoptic-scale influences on Eastern Pacific tropical cyclogenesis. *Mon. Wea. Rev.* **128**, 3296–3307.

Mozer, J. B. and Zhender, J. A. 1996. Lee vorticity production by large-scale tropical mountain ranges. Part I: a mechanism for tropical cyclogenesis in the eastern North Pacific. *J. Atmos. Sci.* **53**, 521–538.

Smith, T. M., Reynolds, R. W., Livezey, R. E. and Stokes, D. C. 1996. Reconstruction of historical sea surface temperatures using empirical orthogonal functions. *J. Climate* **9**, 1403–1420.

Wang, B. and Chan, J. C. L. 2002. How strong ENSO events affect tropical storm activity over the western North Pacific. *J. Climate* **15**, 1643–1658.

Watterson, I. G., Evans, J. L. and Ryan, B. F. 1995. Seasonal and interannual variability of tropical cyclogenesis: diagnostics from large-scale fields. *J. Climate* **8**, 3052–3066.

Whitney, L. D. and Hobgood, J. 1997. The relationship between sea surface temperatures and maximum intensities of tropical cyclones in the eastern North Pacific Ocean. *J. Climate* **10**, 2921–2930.

Wilks, D. S. 1995. *Statistical Methods in the Atmospheric Sciences*, 467 pp, Academic Press, New York.

Zhao, X. and Chu, P.-S. 2006. Bayesian multiple changepoint analysis of hurricane activity in the eastern North Pacific: a Markov chain Monte Carlo approach. *J. Climate* **19**, 564–578.